

The quantum change point

Gael Sentís¹, Emilio Bagan², John Calsamiglia², Giulio Chiribella^{3,4}, and Ramon Muñoz-Tapia²

¹*Departamento de Física Teórica e Historia de la Ciencia,*

Universidad del País Vasco UPV/EHU, E-48080 Bilbao, Spain

²*Física Teòrica: Informació i Fenòmens Quàntics, Departament de Física,*

Universitat Autònoma de Barcelona, 08193 Bellaterra (Barcelona), Spain

³*Department of Computer Science, The University of Hong Kong, Pokfulam Road, Hong Kong*

⁴*Canadian Institute for Advanced Research, CIFAR Program in Quantum Information Science, Toronto, ON M5G 1Z8*

Sudden changes are ubiquitous in nature. Identifying them is crucial for a number of applications in biology, medicine, and social sciences. Here we take the problem of detecting sudden changes to the quantum domain. We consider a source that emits quantum particles in a default state, until a point where a mutation occurs that causes the source to switch to another state. The problem is then to find out where the change occurred. We determine the maximum probability of correctly identifying the change point, allowing for collective measurements on the whole sequence of particles emitted by the source. Then, we devise online strategies where the particles are measured individually and an answer is provided as soon as a new particle is received. We show that these online strategies substantially underperform the optimal quantum measurement, indicating that quantum sudden changes, although happening locally, are better detected globally.

The detection of sudden changes in a sequence of random variables is a pivotal topic in statistics, known as the *change point problem* [1–3]. The problem has widespread applications, including the study of stock market variations [4], protein folding [5], and landscape changes [6]. In general, identifying change points plays a crucial role in all problems involving the analysis of samples collected over time [2, 7] because such analysis requires the stability of the system parameters [8]. If changes are correctly detected, the sample can be conveniently divided in sub-samples, which can then be analyzed by the standard statistical techniques. The detection of change points can also be viewed as a border problem [9], namely a problem where one wants to draw a separation between two (or more) different configurations—a task that plays a central role in machine learning [10].

The simplest example of a change point problem is that of a coin with variable bias. Imagine that a game of Heads or Tails is played with a fair coin, but after a few rounds one player suspects that the other has replaced the coin with a biased one. After inspection of the coin, the suspicion is confirmed: the coin has now a bias. Can we identify when the coin was changed based only on the the sequence of outcomes? This classical problem has a natural extension to the quantum realm, illustrated in Figure 1: A source is promised to prepare quantum particles in some default state. At some point, however, the source undergoes a mutation and starts to produce copies of a different state. Given the sequence of particles emitted by the source, the problem is to find out when the change took place. In the basic version of the problem, the initial and final states are known, as in the classical example of the coin. No prior information is given about the location of the change: a priori, every point of the sequence is equally likely to be the change point. For simplicity, we assume the quantum states to be pure.

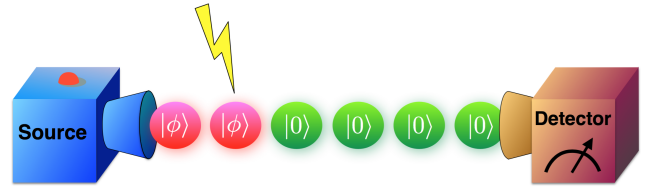


FIG. 1: **The quantum change point problem.** A quantum source emits particles in a default state $|0\rangle$, until the point where a mutation occurs, causing the source to emit particles in a different state $|\phi\rangle$. A detector receives the stream of particles emitted from the source and measures them, producing an estimate of the point where the mutation occurred.

More elaborate variations can be considered, e.g., with unknown states, non-uniform priors, mixed states, and multiple change points. However, as we will see in this Letter, the basic scenario already captures the intriguing features that distinguish the quantum change point problem from its classical version. An example where the change can happen only at two possible positions and the states are completely unknown was studied in [11], where the problem was shown to be equivalent to programmable discrimination [12].

The quantum change point problem can be formulated as a problem of state discrimination. For a sequence of n particles emitted by the source, the problem is to distinguish among n quantum states, the k -th state having the change point in the k -th position. Notably, state discrimination problems with multiple quantum states have no closed-form solution in general (see [13] for some recent progress). A complete solution is known only for the two-state case, a result that dates back to Helstrom’s seminal work four decades ago [4]—and even in this case

computing the success probability may not be straightforward, see, e.g., the derivation of the quantum Chernoff bound [15]. For $n \geq 3$, the only cases where a solution is known are those of pure states with a high degree of symmetry. This includes the symmetric states [16], generated by the action of a unitary operation U satisfying $U^n = \mathbb{1}$, and, more generally, states that are generated by a group of unitaries [17, 18].

Interestingly, the change point problem does not fall into any of the above categories. In spite of this, we show that the problem can be completely solved in the asymptotic regime: in the limit of long sequences, the maximum probability of success takes the elegant form

$$P_{\max} = \frac{4(1-c^2)}{\pi^2} K^2(c^2) + O\left(\frac{1}{n^{1-\epsilon}}\right), \quad (1)$$

where c is the overlap between the default state and the alternate state, $K(x)$ is the complete elliptic function of the first kind [2], and $\epsilon > 0$ is an arbitrary constant. Quite remarkably, the limit probability has a non-zero value despite the fact that the number of states to be distinguished tends to infinity.

Eq. (1) characterizes the ultimate quantum limit to the detection of a change point. Achieving the limit requires a nonlocal measurement, performed jointly on all the particles in the sequence. To perform such measurement one needs a quantum memory, wherein the states received from the source can be stored as they arrive to the detector. Since quantum memories are challenging to implement, it is also interesting to consider local strategies, where the particles are measured as soon as they arrive to the detector, possibly adapting the measurement settings at one step based on the outcomes of the previous measurements steps. Local strategies are interesting also because they can provide an online answer: they have a chance to identify the change point as soon as it occurs, without having to wait until all the n particles are scanned. When the online strategies are compared with the optimal quantum strategy, our results indicate the presence of a gap, showing that the availability of a quantum memory and the ability to perform nonlocal measurements offer an advantage in the identification of the change point.

Let us derive the optimal quantum strategy. We denote by $|0\rangle$ the default state and by $|\phi\rangle = c|0\rangle + s|1\rangle$ the state after the change. Without loss of generality, we choose c to be real and positive. If the change occurs in the position k , the state of the n particles is

$$|\Psi_k\rangle = |0\rangle^{\otimes k-1} |\phi\rangle^{\otimes n-k+1} \quad (2)$$

We call the above states the *source states*. Note that the source states are linearly independent, except in the trivial case when the states $|\phi\rangle$ and $|0\rangle$ are equal. In principle, the change can occur in any position, meaning that every source state has the same *a priori* probability $1/n$ [29].

The detector is described by a positive operator-valued measure (POVM), namely a set of operators $\{M_k\}_{k=1}^n$ satisfying the positivity condition $M_k \geq 0$ and the completeness relation $\sum_{k=1}^n M_k = \mathbb{1}$, where $\mathbb{1}$ denotes the identity in the space \mathcal{S} spanned by the source states. The average probability of successfully identifying the change point is $P = (1/n) \sum_{k=1}^n \langle \Psi_k | M_k | \Psi_k \rangle$ and our goal is to maximize it over all possible POVMs.

As mentioned above, the source states do not fall into any of the categories of states that admit a closed-form solution to the detection problem. Still, we now show how an optimal solution can be constructed in the large n limit. The key to our argument is a general result about the discrimination of linearly independent pure states, which is of independent interest:

Theorem 1 *Let $\{|\Psi_k\rangle\}_{k=1}^n$ be a set of linearly independent states and let*

$$G_{ij} = \langle \Psi_i | \Psi_j \rangle \quad (3)$$

be the components of the corresponding Gram matrix. The maximum probability of correctly identifying a state drawn uniformly at random from the set $\{|\Psi_k\rangle\}_{k=1}^n$ satisfies the bounds

$$P_{\max} \geq \left(\frac{\text{tr} \sqrt{G}}{n} \right)^2 \quad (4)$$

and

$$P_{\max} \leq \left(\frac{\text{tr} \sqrt{G}}{n} \right)^2 + \sqrt{\lambda_{\max}} \|\mathbf{q} - \mathbf{u}\|_1, \quad (5)$$

where λ_{\max} is the maximum eigenvalue of G , $\mathbf{q} = \{q_k\}$ is the probability distribution defined by $q_k := (\sqrt{G})_{kk} / \text{tr}[\sqrt{G}]$, $\mathbf{u} = \{u_k\}$ is the uniform distribution ($u_k = 1/n$ for all k), and $\|\mathbf{q} - \mathbf{u}\|_1 := \sum_k |q_k - u_k|$ is the trace norm.

The proof of Theorem 1 is provided in the Supplemental Material [20], where we further extend the result to non-uniform prior distributions. Note that the two bounds (4) and (5) are exactly equal when the diagonal matrix elements of \sqrt{G} are all equal to each other. In this case, Theorem 1 yields the exact value of the success probability, reproducing a recent result of Ref. [3].

We now evaluate the bounds (4) and (5) for the change point problem, showing that the two bounds match at the leading order. We start by evaluating the trace of \sqrt{G} . First, we observe that the Gram matrix has matrix elements $G_{ij} = c^{|i-j|}$ and that its inverse has the simple form

$$G^{-1} = \frac{1+c^2}{1-c^2} \mathbb{1} - \frac{c}{1-c^2} H, \quad (6)$$

where $H_{ij} = \delta_{ij+1} + \delta_{ji+1} + c(\delta_{i1}\delta_{j1} + \delta_{in}\delta_{jn})$. Luckily, the eigenvalues and eigenvectors of H can be constructed

explicitly: in the Appendix we show that the eigenvalues have the form $2 \cos \theta_l$, where θ_l is a suitable angle in the interval of size π/n centered around $\pi l/n$ [20]. Eq. (6) then implies that the eigenvalues of the Gram matrix G are

$$\lambda_l = \frac{1 - c^2}{1 - 2c \cos \theta_l + c^2}, \quad (7)$$

so that we have

$$\frac{\text{tr} \sqrt{G}}{n} = \frac{1}{n} \sum_{l=1}^n \sqrt{\frac{1 - c^2}{1 - 2c \cos \theta_l + c^2}}. \quad (8)$$

Since the angles θ_l are distributed in intervals of equal size, forming a partition of the interval $[0, \pi)$, the sum can be replaced by an integral in the large n limit, yielding the asymptotic equality

$$\begin{aligned} \frac{\text{tr} \sqrt{G}}{n} &= \frac{\sqrt{1 - c^2}}{\pi} \int_0^\pi \frac{d\theta}{\sqrt{1 - 2c \cos \theta + c^2}} \\ &= \frac{2\sqrt{1 - c^2}}{\pi} K(c^2), \end{aligned} \quad (9)$$

valid up to an error of size $1/n^{1-\epsilon}$ [20]. According to Eq. (4), the square of the r.h.s. is a lower bound for the maximum success probability.

Let us now evaluate the upper bound (5). First, note that we have $\lambda_{\max} \leq (1 + c)/(1 - c)$, as one can easily read out from Eq. (7). Moreover, it is possible to show that the probability distribution \mathbf{q} is approximately uniform, with the bound $\|\mathbf{q} - \mathbf{u}\|_1 \leq 4(1 + c)/(1 - c) 1/n^{1-\epsilon}$ holding at the leading order in n [20]. Hence, the upper bound (5) yields the inequality

$$P_{\max} \leq \left(\text{tr} \sqrt{G}/n \right)^2 + 4 \left(\frac{1 + c}{1 - c} \right)^{3/2} \frac{1}{n^{1-\epsilon}}. \quad (10)$$

In summary, the bounds (4) and (5) match in the asymptotic limit, up to an error of size $1/n^{1-\epsilon}$. This establishes the validity of Eq. (1).

Asymptotically, the maximum success probability is attained by the square root measurement [23, 24]. Indeed, it is possible to show [20] that the success probability of the square root measurement, denoted by P_{SQ} , satisfies the bound

$$P_{\text{SQ}} \geq \left(\text{tr} \sqrt{G}/n \right)^2 \quad (11)$$

and therefore is equal (at the leading order) to the maximum success probability. We also performed a numerical analysis, revealing that the square root measurement is an extremely good approximation already for short sequences ($n \gtrsim 10$), with a difference with respect to the optimal success probability of less than 10^{-3} . In Fig. 2 we compare the asymptotic result in Eq. (1) with the results for $n = 50$ corresponding to the square root measurement and to the optimal measurement obtained via

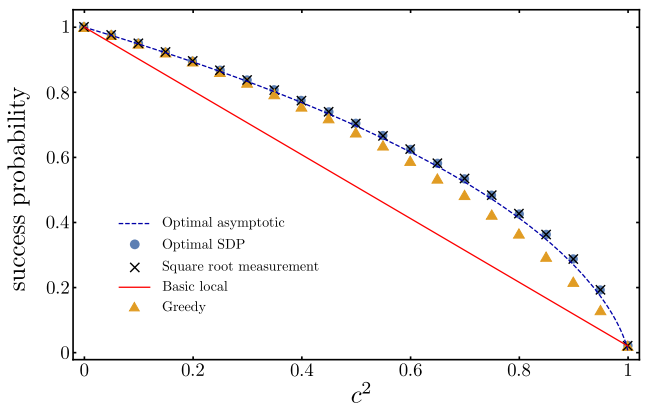


FIG. 2: Probability of correct identification of the change point as a function of $c^2 = |\langle 0|\phi\rangle|^2$. The (blue) dashed line is the asymptotic result in Eq. (1). For a sequence of $n = 50$ states, we also plot the maximum probability, obtained by SDP optimization, (blue) solid dots, and the results corresponding to: the square root measurement, (black) crosses (which lie virtually on top of the dots); the basic local strategy, (red) straight line; and the greedy strategy, (orange) triangles.

Semidefinite Programming [25]. As it is apparent from the figure, the agreement is strikingly good. The figure also includes the success probability of various local measurement strategies that will be discussed below. Notice that for $c = 0$ the source states are orthogonal and perfect identification is possible, while in the limit $c \rightarrow 1$ the source states become indistinguishable and the success probability is given by random guessing, $P_{\max} = 1/n \rightarrow 0$ for $n \rightarrow \infty$. It is also patent from the figure that Eq. (1) is a lower bound that becomes tight as n goes to infinity, in agreement with the bounds (4) and (5). A numerical fit reveals that the correction to the leading order in Eq. (1) is of order $1/n$, again, consistently with our estimate.

Both the optimal measurement and the square root measurement involve global operations on all the n particles. This means that one has to scan the whole sequence of particles before getting an estimate of the change point. We now analyze the performance of online strategies, where each particle is individually measured as soon as it reaches the detector. The simplest such strategy consists in measuring each particle in the computational basis $\{|0\rangle, |1\rangle\}$. The measurements are performed sequentially until the outcome 1 is obtained for the first time, say at the r -th step. At this point, we will know for sure that the measured particle was in the state $|\phi\rangle$, meaning that the change must have occurred at some position $k \leq r$. Our best guess for the change point is then $\hat{k} = r$, since this is the most likely hypothesis given the observed data. For the success probability one has the exact expression $P_{\text{BL}} = 1 - c^2 + c^2/n$, where BL stands for “basic local”. This strategy is suboptimal for $0 < c < 1$, and remains suboptimal for $n \rightarrow \infty$. The

relative difference between the two success probabilities can be of up to 50% for suitable values of the overlap c .

It is intriguing to explore whether more general online strategies can increase the success probability. Let us consider a scenario where a classical learning agent is asked to guess when the change point occurs. The agent starts with a uniform prior $p(k) = 1/n$ about the location of the change point and updates her expectation as new data become available. In order to update her information at the s -th step, the agent must perform a measurement, which generally depends on the results, r_1, r_2, \dots, r_{s-1} obtained in the previous steps. Here we focus on *greedy strategies* [28], i. e. strategies that maximize the success probability at every step [30]. For these strategies, we determine the optimal measurement and the optimal guessing rule. The optimal strategy works as follows: At step s , the agent has to perform the Helstrom measurement [4] that distinguishes between the states $|0\rangle$ and $|\phi\rangle$, given with (unnormalized) prior probabilities [20]

$$\begin{aligned} p_0^{(s)} &:= \max_k \{p(k|r_1, \dots, r_{s-1})\}_{k=s+1}^n \\ p_\phi^{(s)} &:= \max_k \{p(k|r_1, \dots, r_{s-1})\}_{k=1}^s. \end{aligned} \quad (12)$$

Here $p_0^{(s)}$ [$p_\phi^{(s)}$] is the probability of the most likely sequence that has the particle at position s in the state $|0\rangle$ [$|\phi\rangle$]. The agent can deduce these probabilities from the posterior probabilities, updated at step s . After the s -th measurement has been performed, the prior is updated in accordance with the measurement result, using Bayes' update rule: adopting the shorthand notation $\eta_k^{(s)} := p(k|r_1, \dots, r_{s-1})$, we have

$$\eta_k^{(s+1)} = \frac{p(r_s|k) \eta_k^{(s)}}{\sum_{l=1}^n p(r_s|l) \eta_l^{(s)}}. \quad (13)$$

After the last measurement, the agent updates the prior to $\eta_k^{(n+1)}$ and produces the guess \hat{k} that maximizes $\eta_k^{(n+1)}$ for the change point.

For the greedy strategy, the full optimization over the measurements has been carried out analytically. However, a direct quantification of the average performance is intractable, because the number of possible sequences of outcomes grows exponentially with n . In order to compute the average success probability we used a Monte Carlo simulation, leading to the values plotted in Fig. 2 (orange triangles). The figure shows a significant enhancement of performance over the basic local strategy. Still, the optimal greedy strategy does *not* attain the optimal quantum performance, as the gap with the optimal collective strategy remains even for large values of n . In short, this means that a learner with quantum memory outperforms a (greedy) learner with classical memory in the task of detecting change points.

Having observed a gap between the optimal greedy strategy and the optimal quantum strategy, it is interesting to check whether the gap can be closed by using arbitrary local strategies, where each particle can be measured multiple times and the measurement settings can depend on the outcomes of all previous measurements. Note that here the learner is allowed to use a quantum memory, but is limited to perform individual measurements on the particles. Unfortunately, optimizing over arbitrary local strategies is a daring task. Nevertheless, we can provide an upper bound to the success probability by considering POVM operators that are positive under partial transposition (PPT). In this case, a numerical optimization proves the existence of a gap between the local strategies and the optimal collective strategy for every value of n up to $n = 7$.

In this Letter we introduced the quantum change point problem—a quantum version of the problem of identifying changes in a sequence of random variables. In the quantum change point problem, a source emits particles in a default state until a point where a mutation occurs, causing the source to switch to a different state. For pure states, we determined the maximum probability of correctly identifying the change point, showing that, for large sequences of particles, the optimal performance is attained by the square root measurement. We also investigated online strategies, where each particle is measured individually as soon as it is received from the source. Among the online strategies, we identified the optimal greedy strategy, which provides the best online guess at each step. Our calculations show a gap between the greedy strategy and the optimal quantum strategy based on a global measurement. Further numerical optimization shows that the gap remains open even for arbitrary local strategies, indicating that local operations cannot match the performance of the optimal quantum protocol. In particular, this shows that a machine with quantum memory can outperform all machines with classical memory.

Acknowledgments. This research was supported by the Spanish MINECO through contracts FIS2013-40627-P & FIS2015-67161-P, the ERC Starting Grant 258647/GEDENTQOPT, the Generalitat de Catalunya CIRIT contract 2014-SGR966, the Foundational Questions Institute (FQXi- RFP3-1325 and FQXi-MGA-1502), the National Natural Science Foundation of China through Grant No. 11675136, the Hong Kong Research Grant Council through Grant No. 17326616, the Canadian Institute for Advanced Research, the Young 1000 Talents Program of China, and the HKU Seed Funding for Basic Research.

[1] E.S. Page, *Biometrika* **1**, 100 (1954); *ibid* **44**, 523 (1955).

- [2] B.E. Brodsky and B.S. Darkhovsky, *Non-Parametric Statistical Diagnosis* (Springer-Science+Business Media, B.V, Dordrecht, 2000).
- [3] M. Baseville and I.V. Nikiforov, *Detection of Abrupt Changes: Theory and Application* (Prentice Hall information and system sciences series, New Jersey, 1993).
- [4] J. Chen and A. K. Gupta, *Journal of the American Statistical Association* **92**, 438 (1997).
- [5] M. Pirchi, G. Ziv, I. Riven, S. Sedghani Cohen, N. Zohar, Y. Barak, and G. Haran, *Nature Communications* **2**, 493 (2011).
- [6] G. Francesco Ficetola and M. Denoel, *Ecography* **32** 1075 (2009).
- [7] J. Chen and A.K. Gupta, *Parametric Statistical Change Point Analysis, 2nd Ed.* (Birkhäuser, Boston, 2012).
- [8] D.M. Hawkins, *Journal of Royal Statistical Society Series C* **25**, 51 (1976).
- [9] E. Rosten, R. Porter and T. Drummond, *IEEE Transactions on Pattern Analysis and Machine Intelligence*, **32** 105 (2010).
- [10] J. Takeuchi and K. Yamanishi, *IEEE Transactions on Knowledge and Data Engineering* **18**, 482 (2006).
- [11] D. Akimoto and M. Hayashi, *Phys. Rev. A* **83**, 052328 (2011).
- [12] G. Sentis, E. Bagan, J. Calsamiglia, and R. Muñoz-Tapia *Phys. Rev. A* **82**, 042312 (2010); *ibid.* Erratum *Phys. Rev. A* **83**, 039909 (2011).
- [13] K. Nakahira, K. Kato and T.S. Usuda, *Phys. Rev. A* **91**, 052304 (2015).
- [14] C.W. Helstrom, *Quantum Detection and Estimation Theory* (Academic Press, New York, 1976).
- [15] K.M.R. Audenaert et al. *Phys. Rev. Lett.* **98**, 160501 (2007); J. Calsamiglia et al. *Phys. Rev. A* **77**, 032311 (2008).
- [16] S. M. Barnett, *Phys. Rev. A* **64**, 030303R (2001).
- [17] G. Chiribella, G.M. D’Ariano, P. Perinotti, and M.F. Sacchi, *Phys. Rev. A* **70**, 062105 (2004).
- [18] G. Chiribella, G. M. D’Ariano, P. Perinotti, and M. F. Sacchi, *Int. J. Quant. Inf.* **4**, 453 (2005).
- [19] M. Abramowitz and I.A. Stegun, *Handbook of Mathematical Functions* (Dover, New York, 1970).
- [20] See Supplemental Material.
- [21] V. P. Belavkin, *Stochastics* **1**, 315 (1975).
- [22] N. Dalla Pozza and G. Pierobon, *Phys. Rev. A* **91**, 042334 (2015).
- [23] P. Hausladen and W. K. Wootters, *J. Mod. Opt.* **41**, 2385 (1994).
- [24] P. Hausladen, R. Jozsa, B. Schumacher, M. Westmoreland, and W.K. Wootters, *Phys. Rev. A* **54**, 1869 (1996).
- [25] S. Boyd and L. Vanderberghe, *Convex Optimization* (Cambridge University Press, Cambridge, 2004).
- [26] R.E. Bellman, *Dynamic Programming* (Princeton University Press, Princeton 2010).
- [27] J. Calsamiglia, J. I. de Vicente, R. Muñoz-Tapia, and E. Bagan, *Phys. Rev. Lett.* **105**, 080504 (2010).
- [28] P.E. Black, “Greedy Algorithm”, in *Dictionary of Algorithms and Data Structures* [online], Vreda Pieterse and Paul E. Black, eds. (2005).
- [29] It is easy to include the case where the change does not occur at all, by adding the vector $|\Psi_0\rangle = |0\rangle^{\otimes n}$ and replacing the probability with $1/(n+1)$.
- [30] In the considered scenario, the most general strategy can be optimized by dynamical programming, an optimization technique based on backward induction [26]. Unfor-

tunately, for the change point, the numerical overhead is prohibitive, as one needs to accurately approximate n -multidimensional functions. In practice, such technique is only suitable for problems with a limited number of hypothesis [27].

SUPPLEMENTAL MATERIAL

Proof of theorem 1 and generalization to arbitrary priors

Here we provide a lower and an upper bound on the probability of correct state discrimination, valid for a generic set of linearly independent pure states $\{|\Psi_k\rangle\}_{k=1}^n$ and for a generic choice of prior probabilities $\{p_k\}_{k=1}^n$. The bounds are expressed in terms of the Gram matrix of the weighted states

$$|\tilde{\Psi}_k\rangle := \sqrt{p_k} |\Psi_k\rangle, \quad (14)$$

that is, the matrix W with elements

$$W_{ij} := \langle \tilde{\Psi}_i | \tilde{\Psi}_j \rangle. \quad (15)$$

The maximum success probability can be estimated with the following Theorem, which generalizes Theorem 1 of the main text to arbitrary prior distributions:

Theorem 2 *Let $\{|\Psi_k\rangle\}_{k=1}^n$ be a set of linearly independent pure states. The maximum probability of correctly identifying a state drawn from the set $\{|\Psi_k\rangle\}_{k=1}^n$ with probability $\{p_k\}_{k=1}^n$ satisfies the bounds*

$$P_{\max} \geq \frac{(\text{tr} \sqrt{W})^2}{n} \quad (16)$$

and

$$P_{\max} \leq \frac{(\text{tr} \sqrt{W})^2}{n} + \sqrt{n \lambda_{\max}} \|\mathbf{q} - \mathbf{u}\|_1, \quad (17)$$

where λ_{\max} is the maximum eigenvalue of W , $\mathbf{q} = \{q_k\}$ is the probability distribution defined by $q_k := (\sqrt{W})_{kk} / \text{tr}(\sqrt{W})$, $\mathbf{u} = \{u_k\}$ is the uniform distribution, and $\|\mathbf{q} - \mathbf{u}\|_1 := \sum_k |q_k - u_k|$ is the trace norm.

Proof. Since the states $\{|\Psi_k\rangle\}_{k=1}^n$ are linearly independent, the optimal measurement consists of orthogonal rank-one projectors [1]. Let us denote the projectors by $M_k = |m_k\rangle\langle m_k|$, for a suitable orthonormal basis $\{|m_k\rangle\}_{k=1}^n$. Then, the probability of correct discrimination can be written as

$$\begin{aligned} P_{\text{succ}} &= \sum_k p_k |\langle m_k | \Psi_k \rangle|^2 \\ &= \sum_k |\langle m_k | \tilde{\Psi}_k \rangle|^2 \\ &= \sum_k |B_{kk}|^2, \end{aligned} \quad (18)$$

where B is the matrix defined by the relation

$$|\tilde{\Psi}_k\rangle = \sum_i B_{ik} |m_i\rangle. \quad (19)$$

By definition, one has $B^\dagger B = W$. Hence, the polar decomposition yields the relation

$$B = U\sqrt{W}, \quad (20)$$

for a suitable unitary matrix U . Note that a generic change of orthonormal basis,

$$|m_i\rangle \rightarrow |m'_i\rangle = \sum_j V_{ji} |m_j\rangle \quad (21)$$

(where V is a generic unitary matrix), results into the change of matrix

$$B \rightarrow B' = V^\dagger B. \quad (22)$$

Combining Eqs. (20) and (22), the maximum probability of correct discrimination can be expressed as

$$P_{\max} = \max_U \sum_k \left| \left(U\sqrt{W} \right)_{kk} \right|^2. \quad (23)$$

Setting $U = \mathbb{1}$, one has the lower bound

$$P_{\max} \geq \sum_k \left(\sqrt{W} \right)_{kk}^2 \geq \frac{(\text{tr } \sqrt{W})^2}{n}, \quad (24)$$

the second inequality following from the convexity of the function $f(x) = x^2$. This proves the lower bound (16).

Let us prove the upper bound (17). Using the Cauchy-Schwarz inequality in Eq. (23), we obtain the upper bound

$$\begin{aligned} P_{\max} &= \max_U \sum_k \left| \sum_s \left(UW^{\frac{1}{4}} \right)_{ks} \left(W^{\frac{1}{4}} \right)_{sk} \right|^2 \\ &\leq \max_U \sum_k \left(\sqrt{W} \right)_{kk} \left(U\sqrt{W}U^\dagger \right)_{kk} \\ &= \text{tr} \left(\sqrt{W} \right) \times \max_U \left[\sum_k q_k \left(U\sqrt{W}U^\dagger \right)_{kk} \right]. \end{aligned}$$

Moreover, the argument of the maximum can be upper bounded as

$$\begin{aligned} \sum_k q_k \left(U\sqrt{W}U^\dagger \right)_{kk} &\leq \sum_k \frac{1}{n} \left(U\sqrt{W}U^\dagger \right)_{kk} \\ &\quad + \sum_k \left| q_k - \frac{1}{n} \right| \left(U\sqrt{W}U^\dagger \right)_{kk} \\ &\leq \frac{\text{tr } \sqrt{W}}{n} + \|\mathbf{q} - \mathbf{u}\|_1 \sqrt{\lambda_{\max}}. \end{aligned}$$

Finally, from Eq. (16) we have the bound

$$\text{tr } \sqrt{W} \leq \sqrt{n P_{\max}} \leq \sqrt{n}. \quad (25)$$

Combining the above inequalities we obtain the desired upper bound (17). ■

When the prior distribution is uniform, the weighted Gram matrix W is given by $W = G/n$, where G is the unweighted Gram matrix used in the main text. Substituting this relation into the bound (17) one obtains Eq. (5) of the main text.

Eigenvalues and eigenvectors of H

In this section we derive explicit expressions for the eigenvectors and eigenvalues of the matrix H .

To this purpose, it is useful to first recall some properties of the Chebyshev polynomials of the second kind, denoted by $U_n(x)$. The Chebyshev polynomials of the second kind can be defined as the characteristic polynomial of the tridiagonal matrix T of size n whose entries are $T_{ij} = \delta_{i,j+1} + \delta_{j,i+1}$. Specifically, $U_n(x) = \det(2x\mathbb{1} - T)$, i.e., the eigenvalues of T are defined to be twice the roots, x_l , of $U_n(x)$. By expanding the determinant by the first row one readily obtains the well known recursion relation $U_n(x) = 2xU_{n-1}(x) - U_{n-2}(x)$ [2]. One can check that this recursion relation along with the initial conditions in standard form, $U_0(x) = 1$, $U_{-1}(x) = 0$, give the right characteristic polynomial for *any* size of T . It suffices to check the $n = 1, 2$ cases. One has $U_1(x) = 2x$ and $U_2(x) = 4x^2 - 1$, which are indeed the characteristic polynomials of T of sizes 1 and 2.

We now turn to the eigenvalues and eigenvectors of H , which we will compute using a different approach. The matrix H is nothing but the matrix T with the addition of two extra entries at each end of the principal diagonal, namely, $H_{ij} = T_{ij} + c(\delta_{i1}\delta_{j1} + \delta_{in}\delta_{jn})$. Let us denote by $2x_l$ the l -th eigenvalue of H and by \mathbf{w}^l the corresponding unnormalized eigenvector, chosen with the convention $w_1^l = 1$. The equation $H\mathbf{w}^l = 2x_l\mathbf{w}^l$ is equivalent to the following system of linear equations:

$$\begin{aligned} cw_1^l + w_2^l &= 2x_l w_1^l; \\ w_{j-1}^l + w_{j+1}^l &= 2x_l w_j^l, \quad 2 \leq j \leq n-1; \\ w_{n-1}^l + cw_n^l &= 2x_l w_n^l. \end{aligned} \quad (26)$$

The second line of this system can be viewed as the recursion relation $w_{j+1}^l = 2x_l w_j^l - w_{j-1}^l$, which is the recursion relation of the Chebyshev polynomials given above (with $n \rightarrow j+1$). It follows that the first and second line of Eq. (26), along with the convention $w_1^l = 1$, imply

$$w_j^l = U_{j-1}(x_l) - cU_{j-2}(x_l), \quad j = 1, 2, \dots, n. \quad (27)$$

Since all the components of \mathbf{w}^l have been determined, the third line in Eq. (26) must give the eigenvalues of H .

By substituting Eq. (27) in the third line of Eq. (26) and using the Chebyshev recursion relation again, one obtains

$$0 = U_n(x_l) - 2cU_{n-1}(x_l) + c^2U_{n-2}(x_l) := P_n(x_l), \quad (28)$$

which must hold for $l = 1, \dots, n$. The polynomial $P_n(x)$ has degree n and its n roots, x_l , give the eigenvalues of H as $2x_l$. Note that $P_n(x)$ has to be proportional to the characteristic polynomial of H , i.e., $P_n(x) \propto \det(2x\mathbb{1} - H)$, as both polynomials have the same degree and the same zeroes.

Distribution of the eigenvalues of H

Here we analyze the distribution of the zeroes of the polynomial $P_n(x)$ defined in Eq. (28).

Setting $x = \cos \theta$, we recall that the Chebyshev polynomial $U_n(\cos \theta)$ can be expressed as [2]

$$U_n(\cos \theta) = \frac{\sin(n+1)\theta}{\sin \theta}. \quad (29)$$

Then, a little bit of trigonometry yields the relation

$$P_n(\cos \theta) = A(\theta) \sin[n\theta + \delta(\theta)], \quad (30)$$

with

$$\begin{cases} A(\theta) := \frac{1 - 2c \cos \theta + c^2}{\sin \theta} \\ \delta(\theta) := \arctan \frac{(1 - c^2) \sin \theta}{(1 + c^2) \cos \theta - 2c} \end{cases}, \quad (31)$$

where $0 < \delta(\theta) < \pi$. From Eq. (30) we can see that every zero of $P_n(\cos \theta)$ must be the solution to one of the equations

$$n\theta + \delta(\theta) = l\pi, \quad l = 1, 2, \dots, n. \quad (32)$$

Denote by θ_l the angle that solves the l -th equation. Since $\delta(\theta_l)$ is contained in the interval $(0, \pi)$, we have the bound

$$\frac{\pi}{n}l \leq \theta_l \leq \frac{\pi}{n}(l+1). \quad (33)$$

In other words, the interval $(0, \pi)$ can be divided into intervals of length π/n , with the l -th interval containing the zero θ_l . For large n , this means that the zeros are uniformly distributed in the interval $(0, \pi)$.

The trace and diagonal matrix elements of \sqrt{G}

Here we evaluate the normalized trace \sqrt{G}/n and we quantify its deviation from the limit value $\gamma := \lim_{n \rightarrow \infty} \text{tr} \sqrt{G}/n$. In the process of computing the trace, we also evaluate the diagonal matrix elements of \sqrt{G} , which will become useful in the next section.

We proceed along the following steps:

1. construct the normalized eigenvectors of \sqrt{G}
2. evaluate the diagonal elements
3. evaluate the trace.

The normalized eigenvectors of \sqrt{G}

The eigenvectors of \sqrt{G} coincide with the eigenvectors of the matrix H , provided in Eq. (27). Setting $x_l = \cos \theta_l$, we can use the trigonometric representation of the Chebyshev polynomials given in Eq. (29). In this way, we obtain

$$w_j^l = \frac{\sin(j\theta_l) - c \sin[(j-1)\theta_l]}{\sin \theta_l}. \quad (34)$$

Now, the norm \mathbf{w}^l can be evaluated explicitly as

$$\begin{aligned} \|\mathbf{w}^l\|^2 &:= \sum_j |w_j^l|^2 \\ &= \frac{n}{2 \sin^2 \theta_l} \left\{ 1 - 2c \cos \theta_l + c^2 \right. \\ &\quad \left. + \frac{1 - c^2}{2n} [1 - \cos(2n\theta_l)] \right. \\ &\quad \left. - \frac{\sin(2n\theta_l)}{2n \sin \theta_l} [(1 + c^2) \cos \theta_l - 2c] \right\} \\ &= \frac{n}{2 \sin^2 \theta_l} \left\{ 1 - 2c \cos \theta_l + c^2 + \frac{f_n(\theta_l)}{n} \right\}, \end{aligned} \quad (35)$$

having defined the function

$$\begin{aligned} f_n(x) &:= \frac{1 - c^2}{2} [1 - \cos(2nx)] \\ &\quad - \frac{\sin(2nx)}{2 \sin x} [(1 + c^2) \cos x - 2c]. \end{aligned} \quad (36)$$

Defining the normalized eigenvectors $\mathbf{v}^l := \mathbf{w}^l / \|\mathbf{w}^l\|$, we then have

$$|v_j^l|^2 = \frac{2}{n} \frac{[\sin(j\theta_l) - c \sin(j-1)\theta_l]^2}{1 - 2c \cos \theta_l + c^2 + f_n(\theta_l)/n}. \quad (37)$$

The diagonal elements of \sqrt{G}

Having computed the eigenvalues and eigenvectors of the Gram matrix G , we can now evaluate the diagonal elements of its square root \sqrt{G} . We start from the expression

$$\sqrt{G} = \sum_l \sqrt{\lambda_l} |v^l\rangle \langle v^l|, \quad (38)$$

recalling that the eigenvalues are given by

$$\lambda_l = \frac{1 - c^2}{1 - 2c \cos \theta_l + c^2}. \quad (39)$$

Then, the diagonal elements of \sqrt{G} are

$$\left(\sqrt{G}\right)_{kk} = \sum_l \sqrt{\lambda_l} |v_k^l|^2, \quad (40)$$

with v_k^l given as in Eq. (37). Explicitly, the matrix element $(\sqrt{G})_{kk}$ is given by

$$\begin{aligned} \left(\sqrt{G}\right)_{kk} &= \frac{1}{n} \sum_l \sqrt{\frac{1-c^2}{1-2c\cos\theta_l+c^2}} \\ &\times \frac{[\sin k\theta_l - c\sin(k-1)\theta_l]^2}{1-2c\cos\theta_l+c^2+f_n(\theta_l)/n} \end{aligned} \quad (41)$$

We now show that most of the matrix elements $(\sqrt{G})_{kk}$ are approximately equal to the limit value $\gamma := \lim_{n \rightarrow \infty} \text{tr} \sqrt{G}/n$. Note that γ can be computed explicitly in terms the eigenvalues: indeed, one has

$$\begin{aligned} \gamma &= \lim_{n \rightarrow \infty} \frac{1}{n} \sum_l \sqrt{\lambda_l} \\ &= \lim_{n \rightarrow \infty} \frac{1}{n} \sum_l \sqrt{\frac{1-c^2}{1-2c\cos\theta_l+c^2}} \\ &= \frac{1}{\pi} \int_0^\pi d\theta \sqrt{\frac{1-c^2}{1-2c\cos\theta+c^2}}. \end{aligned} \quad (42)$$

We now show that the deviation vanishes for all values of k in the interval $[n^\epsilon, n - n^\epsilon]$. To this purpose, we evaluate the matrix element $(\sqrt{G})_{kk}$ at the leading order of the large n asymptotics, obtained by replacing the sum in Eq. (41) by an integral and by dropping the term $f_n(\theta_l)/n$ in the denominator. In this way, we obtain the approximate equality

$$\left(\sqrt{G}\right)_{kk} \approx \frac{\sqrt{1-c^2}}{\pi} \int_0^\pi d\theta \frac{[\sin k\theta - c\sin(k-1)\theta]^2}{(1-2c\cos\theta+c^2)^{3/2}}. \quad (43)$$

Then, some elementary algebra gives

$$\left(\sqrt{G}\right)_{kk} - \gamma \approx \frac{\sqrt{1-c^2}}{\pi} (2cI_{2k-1} - I_{2k} - c^2 I_{2k-2}), \quad (44)$$

where the integrals I_r are defined as

$$I_r := \int_0^\pi \frac{\cos r\theta d\theta}{(1-2c\cos\theta+c^2)^{3/2}}. \quad (45)$$

We then show that the integrals I_r vanish exponentially with r :

Proposition 1 *For $c < 1$, the leading order of the integral I_r in Eq. (45) is given by*

$$I_r = \frac{2c^r \sqrt{\pi r}}{(1-c^2)^{3/2}}. \quad (46)$$

The proof can be found in the end of this subsection. Inserting the asymptotic expression (46) into Eq. (44) we obtain the relation

$$\left(\sqrt{G}\right)_{kk} - \gamma \approx \frac{1}{4(1-c^2)} \frac{c^{2k}}{\sqrt{2\pi k^3}}, \quad (47)$$

valid in the interval $[n^\epsilon, n - n^\epsilon]$. In conclusion, the deviation $(\sqrt{G})_{kk} - \gamma$ decays exponentially with k . We stress that the error introduced by the approximation (43) is negligible with respect to the leading order, quantified by the r.h.s. of Eq. (47). This point is illustrated in Fig. 3, which compares the the r.h.s. of Eq. (47) with the exact values of the deviation, computed by direct numerical evaluation of \sqrt{G} from G . Log-scale plots are shown for various values of the overlap c , setting $n = 30$ and letting k vary from 1 to 15. The agreement is extremely good and backs up the validity of the approximation (43) even for small values of k .

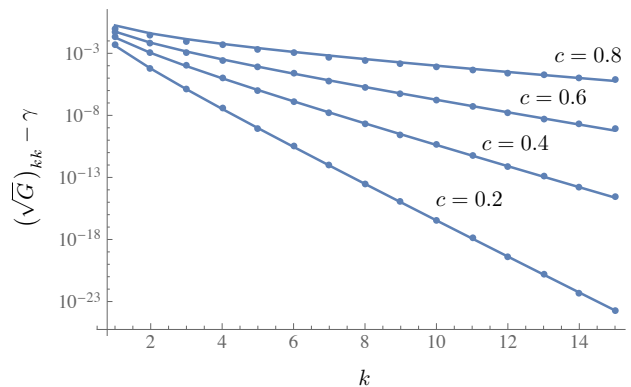


FIG. 3: Log-scale plots of the deviation $(\sqrt{G})_{kk} - \gamma$, for $n = 30$ and k varying from 1 to 15. The solid lines are the asymptotic approximation on r.h.s of Eq. (47) and the dots are the result of numerical evaluation of \sqrt{G} from G .

In the next subsection we will use Eq. (47) to quantify the deviation between the diagonal of the matrix $\sqrt{G}/\text{tr}(\sqrt{G})$ and the uniform distribution.

Proof of Proposition 1. We start by noticing that the integral on the r.h.s of Eq. (45) can be expressed as a contour integral over the unit circle C on the complex plane:

$$I_r = \frac{1}{2i} \oint_C dz \frac{z^{r+1/2}}{[z - c(z^2 + 1) + c^2 z]^{3/2}}. \quad (48)$$

We can choose the branch of the integrand so that its branch cuts are the intervals $[0, c]$ and $[c^{-1}, \infty)$ on the real axis. Since this branch is analytic elsewhere and the cut $[c^{-1}, \infty)$ is outside C , we can deform the contour C to a new contour C' around $[0, c]$. One readily sees that the integrand in Eq. (48) behaves as $(z-c)^{-3/2}$, so care must

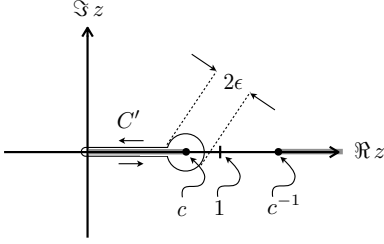


FIG. 4: The figure shows (gray) the branch cuts of the integrand in Eq. (48) and the contour C' used to obtain Eq. (49).

be taken to evaluate the new contour integral near the end point $z = c$, as some divergencies may arise because of this singular behavior. Specifically, we choose C' as in Fig. 4, where $\epsilon > 0$ and the limit $\epsilon \rightarrow 0$ is implicit. As a result, I_r has a contribution coming from the discontinuity of the integrand along the interval $[0, c - \epsilon]$ and a contribution coming from the integration around the circle C_ϵ of radius ϵ and center at $z = c$:

$$I_r = -\frac{1}{c^{3/2}} \int_0^{c-\epsilon} dx \frac{x^{r+1/2}}{\{(c-x)[(1/c)-x]\}^{3/2}} + \frac{1}{2ic^{3/2}} \oint_{C_\epsilon} dz \frac{c^{r+1/2}}{(z-c)^{3/2}[(1/c)-c]^{3/2}}. \quad (49)$$

Note that the limit $\epsilon \rightarrow 0$ of each separate line is ill-defined, as they both diverge as $\epsilon^{-1/2}$. To circumvent this problem, we write $(c-x)^{-3/2} = 2(d/dx)(c-x)^{-1/2}$ and integrate the first line of Eq. (49) by parts. In doing so, we see that the $\epsilon^{-1/2}$ terms cancel and we obtain the simple expression

$$I_r = 2 \int_0^c \frac{dx}{(c-x)^{1/2}} \frac{d}{dx} \frac{x^{r+1/2}}{[1-cx]^{3/2}}. \quad (50)$$

We can further simplify this expression using the change of variable $x = ct$, which enables us to express I_r in terms of hypergeometric functions. However, we are just interested in the asymptotic behavior of I_r . Keeping only the leading contribution as r goes to infinity, we have

$$I_r = 2rc^r \int_0^1 dt t^{r-1/2} (1-t)^{-1/2} (1-c^2t)^{-3/2}. \quad (51)$$

The asymptotic behaviour of this integral can be easily evaluated by noticing that the leading contribution comes from the region near the upper limit of integration, so we

can set $t = 1$ in the last factor in Eq. (51) and write

$$I_r = \frac{2rc^r}{(1-c^2)^{3/2}} \int_0^1 dt t^{r-1/2} (1-t)^{-1/2} = \frac{2rc^r B(\frac{1}{2}, r+\frac{1}{2})}{(1-c^2)^{3/2}} = \frac{2\sqrt{\pi}c^r \Gamma(r+\frac{1}{2})}{(r-1)!(1-c^2)^{3/2}}, \quad (52)$$

where $B(a, b)$ is the Euler Beta function,

$$B(a, b) = \int_0^1 dt t^{a-1} (1-t)^{b-1}, \quad (53)$$

and we have used the relation,

$$B(a, b) = \frac{\Gamma(a)\Gamma(b)}{\Gamma(a+b)}. \quad (54)$$

Using the Stirling formula in the third line of Eq. (52), we finally obtain Eq. (46). ■

The trace of \sqrt{G}

Here we show that the normalized trace $\text{tr} \sqrt{G}/n$ is close to its limit value γ , up to an error of size $1/n^{1-\epsilon}$, where ϵ is an arbitrary constant in the interval $(0, 1)$. For this purpose, we divide the values of k into two subsets, defined as

$$\mathcal{S} := \{k \in \mathbb{N} : [n^\epsilon] \leq k \leq n - [n^\epsilon]\} \\ \bar{\mathcal{S}} := \{1, \dots, n\} \setminus \mathcal{S}. \quad (55)$$

The trace of \sqrt{G} can be evaluated as

$$\text{tr} \sqrt{G} = \sum_{k \in \mathcal{S}} (\sqrt{G})_{kk} + \sum_{k \in \bar{\mathcal{S}}} (\sqrt{G})_{kk} = \sum_{k \in \mathcal{S}} \left(\gamma + \frac{1}{4(1-c^2)} \frac{c^{2k}}{\sqrt{2\pi k^3}} \right) + \sum_{k \in \bar{\mathcal{S}}} (\sqrt{G})_{kk} = |\mathcal{S}| \gamma + \sum_{k \in \bar{\mathcal{S}}} (\sqrt{G})_{kk} + O(n^{1-3\epsilon/2} c^{2n^\epsilon}), \quad (56)$$

the second equality following from Eq. (47).

Using the above expression it is easy to produce upper and lower bounds on $\text{tr} \sqrt{G}$. An upper bound is obtained as follows:

$$\text{tr} \sqrt{G} \leq |\mathcal{S}| \gamma + \sqrt{\lambda_{\max}} |\bar{\mathcal{S}}| + O(n^{1-3\epsilon/2} c^{2n^\epsilon}) \leq n \gamma + \sqrt{\lambda_{\max}} |\bar{\mathcal{S}}| + O(n^{1-3\epsilon/2} c^{2n^\epsilon}). \quad (57)$$

Similarly, we have the lower bound

$$\text{tr} \sqrt{G} \geq |\mathcal{S}| \gamma + O(n^{1-3\epsilon/2} c^{2n^\epsilon}) = n \gamma - \gamma |\bar{\mathcal{S}}| + O(n^{1-3\epsilon/2} c^{2n^\epsilon}). \quad (58)$$

Using the relation $2n^\epsilon \leq |\bar{\mathcal{S}}| \leq 2(n^\epsilon + 1)$ we finally obtain the bounds

$$\gamma - \frac{2\gamma}{n^{1-\epsilon}} \leq \frac{\text{tr} \sqrt{G}}{n} \leq \gamma + 2\sqrt{\lambda_{\max}} \left(\frac{1}{n^{1-\epsilon}} + \frac{1}{n} \right), \quad (59)$$

valid up to an exponentially small correction of size $O(n^{-3\epsilon/2}c^{2n^\epsilon})$. More compactly, the above bounds can be written as

$$\left| \frac{\text{tr} \sqrt{G}}{n} - \gamma \right| \leq \frac{2 \max\{\gamma, \sqrt{\lambda_{\max}}\}}{n^{1-\epsilon}} + O\left(\frac{1}{n}\right). \quad (60)$$

Now, direct inspection shows that $\sqrt{\lambda_{\max}}$ is always larger than γ . Hence, the bound becomes

$$\left| \frac{\text{tr} \sqrt{G}}{n} - \gamma \right| \leq \frac{2\sqrt{\lambda_{\max}}}{n^{1-\epsilon}} + O\left(\frac{1}{n}\right). \quad (61)$$

Deviation of \mathbf{q} from the uniform distribution

In this section we consider the probability distribution $\mathbf{q} = \{(\sqrt{G})_{kk}/\text{tr} \sqrt{G}\}$ for the change point problem and we quantify the deviation of \mathbf{q} from the uniform distribution.

Here we upper bound the trace distance between the probability distribution $\mathbf{q} = \{q_k\}$ defined by

$$q_k := \frac{(\sqrt{G})_{kk}}{\text{tr} \sqrt{G}}$$

and the uniform distribution, denoted by \mathbf{u} . Our strategy is to separately analyze the contributions to the trace distance coming from the two sets \mathcal{S} and $\bar{\mathcal{S}}$ defined in Eq. (55).

Let us consider first the contribution of the set \mathcal{S} . For $k \in \mathcal{S}$, we have

$$\begin{aligned} \left| q_k - \frac{1}{n} \right| &= \left| \frac{(\sqrt{G})_{kk} - \text{tr} \sqrt{G}/n}{\text{tr} \sqrt{G}} \right| \\ &\leq \frac{\left| (\sqrt{G})_{kk} - \gamma \right| + \left| \gamma - \text{tr} \sqrt{G}/n \right|}{\text{tr} \sqrt{G}}. \end{aligned} \quad (62)$$

Now, the first term is upper bounded as

$$\begin{aligned} \left| (\sqrt{G})_{kk} - \gamma \right| &\leq \frac{1}{4(1-c^2)} \frac{c^{2n^\epsilon}}{\sqrt{2\pi n^{3\epsilon}}} \\ &= O\left(n^{-3\epsilon/2}c^{2n^\epsilon}\right), \end{aligned} \quad (63)$$

due to Eq. (47). The second term is upper bounded by Eq. (61). Hence, the contribution of \mathcal{S} to the trace

distance can be upper bounded as

$$\begin{aligned} \sum_{k \in \mathcal{S}} \left| q_k - \frac{1}{n} \right| &\leq \sum_{k \in \mathcal{S}} \frac{2\sqrt{\lambda_{\max}}/n^{1-\epsilon} + O(1/n)}{\text{tr} \sqrt{G}} \\ &\leq \sum_{k \in \mathcal{S}} \frac{2\sqrt{\lambda_{\max}}/n^{1-\epsilon} + O(1/n)}{n\sqrt{\lambda_{\min}}} \\ &\leq \sqrt{\frac{\lambda_{\max}}{\lambda_{\min}}} \frac{2}{n^{1-\epsilon}} + O\left(\frac{1}{n}\right), \end{aligned}$$

having used the relation

$$\text{tr} \sqrt{G} \geq n \sqrt{\lambda_{\min}}, \quad (64)$$

where λ_{\min} is the minimum eigenvalue of G . In conclusion, Eq. (64) shows that the contribution of the set \mathcal{S} vanishes in the large n limit.

Let us consider the contribution of the set $\bar{\mathcal{S}}$. For $k \in \bar{\mathcal{S}}$, we have the inequality

$$\begin{aligned} \left| q_k - \frac{1}{n} \right| &= \left| \frac{(\sqrt{G})_{kk} - \text{tr} \sqrt{G}/n}{\text{tr} \sqrt{G}} \right| \\ &\leq \frac{\sqrt{\lambda_{\max}}}{\text{tr} \sqrt{G}} \\ &\leq \sqrt{\frac{\lambda_{\max}}{\lambda_{\min}}} \frac{1}{n}, \end{aligned} \quad (65)$$

which leads to the upper bound

$$\sum_{k \in \bar{\mathcal{S}}} \left| q_k - \frac{1}{n} \right| \leq \sqrt{\frac{\lambda_{\max}}{\lambda_{\min}}} \frac{2}{n^{1-\epsilon}}. \quad (66)$$

Using the bounds (64) and (66), the deviation between \mathbf{q} and the uniform distribution can be upper bounded as

$$\begin{aligned} \|\mathbf{q} - \mathbf{u}\|_1 &= \sum_{k \in \mathcal{S}} \left| q_k - \frac{1}{n} \right| + \sum_{k \in \bar{\mathcal{S}}} \left| q_k - \frac{1}{n} \right| \\ &\leq \sqrt{\frac{\lambda_{\max}}{\lambda_{\min}}} \frac{4}{n^{1-\epsilon}} + O\left(\frac{1}{n}\right) \\ &\leq \frac{1+c}{1-c} \frac{4}{n^{1-\epsilon}} + O\left(\frac{1}{n}\right), \end{aligned} \quad (67)$$

having used the bounds

$$\lambda_{\max} \leq (1+c)/(1-c) \quad (68)$$

and

$$\lambda_{\min} \geq (1-c)/(1+c), \quad (69)$$

following from Eq. (39).

Lower bound on the success probability of the square root measurement

For a generic set of linearly independent pure states $\{|\Psi_k\rangle\}_{k=1}^n$ and a generic choice of prior probabilities $\{p_k\}_{k=1}^n$, the success probability of the square root measurement can be expressed as [3]

$$P_{\text{SQ}} = \sum_k \left(\sqrt{W} \right)_{kk}^2. \quad (70)$$

The convexity of the function $f(x) = x^2$ then implies the bound $P_{\text{SQ}} \geq (\text{tr } \sqrt{W})^2/n$.

Greedy strategy and Bayesian updating

Here we show that Bayesian updating gives the optimal greedy strategy introduced in the main text. This follows from the observation that the optimal measurement (and the optimal guess) at step s of the greedy strategy are determined solely by the posterior probability distribution after the measurement at step $s-1$, as will be explicitly shown at the end of this section.

To optimize the greedy strategy, we need to maximize $\mathcal{P}_s^{\text{G}} = \sum_{r=1}^n \eta_r^{(s)} \langle \Psi_r | E_s(r) | \Psi_r \rangle$ over all POVM measurements on particle s , $\{E_s(r)\}_{r=1}^n$. Noticing that the source state $|\Psi_k\rangle$ restricted to particle s is $|\Psi_k\rangle_s = |0\rangle$ for $s < k$, and $|\Psi_k\rangle_s = |\phi\rangle$ for $s \geq k$, the following relations are self evident:

$$\begin{aligned} \mathcal{P}_s^{\text{G}} &= \sum_{r=1}^s \eta_r^{(s)} \langle \phi | E_s(r) | \phi \rangle + \sum_{r=s+1}^n \eta_r^{(s)} \langle 0 | E_s(r) | 0 \rangle \\ &\leq p_\phi^{(s)} \sum_{r=1}^s \langle \phi | E_s(r) | \phi \rangle + p_0^{(s)} \sum_{r=s+1}^n \langle 0 | E_s(r) | 0 \rangle \\ &= p_\phi^{(s)} \langle \phi | \Pi_s(\phi) | \phi \rangle + p_0^{(s)} \langle 0 | \Pi_s(0) | 0 \rangle, \end{aligned} \quad (71)$$

where $p_\phi^{(s)} := \max_r \{\eta_r^{(s)}\}_{r=1}^s$, $p_0^{(s)} = \max_r \{\eta_r^{(s)}\}_{r=s+1}^n$, $\Pi_s(\phi) = \sum_{r=1}^s E_s(r)$, and $\Pi_s(0) = \mathbb{1} - \Pi_s(\phi)$. The inequality is saturated by choosing a new POVM $\{E'_s(r)\}_{r=1}^n$ whose elements are non-zero only in the two positions that maximize the prior probabilities:

$$r_\phi = \operatorname{argmax}_r \{\eta_r^{(s)}\}_{r=1}^s, \quad r_0 = \operatorname{argmax}_r \{\eta_r^{(s)}\}_{r=s+1}^n, \quad (72)$$

so that $E'_s(r_0) = \Pi_s(0)$ and $E'_s(r_1) = \Pi_s(\phi)$. This justifies the choice of priors in Eq. (12) of the main text.

The success probability can now be written in terms of the Helstrom matrix $\Gamma_s = p_\phi^{(s)} |\phi\rangle\langle\phi| - p_0^{(s)} |0\rangle\langle 0|$ as:

$$\begin{aligned} \mathcal{P}_s^{\text{G}} &= p_0^{(s)} + \text{tr}(\Pi_s(\phi)\Gamma_s) \leq p_0^{(s)} + \text{tr}(\Gamma_s^+) \\ &= \frac{1}{2} \left(p_\phi^{(s)} + p_0^{(s)} + \text{tr}|\Gamma_s| \right), \end{aligned} \quad (73)$$

where Γ_s^+ is the positive part of matrix Γ . The inequality is saturated by choosing $\Pi_s(\phi)$ to be the projector onto the positive subspace of Γ [4].

We now show that the optimal measurement and guess at step s of the greedy strategy do not depend on the particular sequence measurement outcomes, but only on the posterior probability distribution after the measurement at step $s-1$. Let us introduce the short-hand notation $\mathbf{r}_s := \{r_1, \dots, r_s\}$ for a sequence of results obtained up to step s . The average success probability at each step s is given by

$$\sum_{k=1}^n \sum_{\mathbf{r}_s} p(\mathbf{r}_s, k) \delta_{k, \hat{k}(\mathbf{r}_s)} \leq \sum_{\mathbf{r}_s} \max_k p(\mathbf{r}_s, k), \quad (74)$$

where $p(\mathbf{r}_s, k)$ is the joint probability of obtaining the sequence \mathbf{r}_s of results and the change point occurring at position k , and $\hat{k}(\mathbf{r}_s) \in \{1, \dots, n\}$ is the decision function that assigns to each \mathbf{r}_s the guessed change point position $k = \hat{k}(\mathbf{r}_s)$. The inequality can be saturated by $\hat{k}(\mathbf{r}_s) = \operatorname{argmax}_k p(\mathbf{r}_s, k)$. Since the source states $|\Psi_k\rangle$ are of product form, we can write

$$p(\mathbf{r}_s, k) = \frac{1}{n} p(\mathbf{r}_{s-1} | k) \langle \Psi_k | E_s(r_s) | \Psi_k \rangle, \quad (75)$$

where we recall that $|\Psi_k\rangle$ restricted to particle s is $|\Psi_k\rangle_s = |0\rangle$ for $s < k$, and $|\Psi_k\rangle_s = |\phi\rangle$ for $s \geq k$. The measurement over the s -th particle is represented by the POVM $\{E_s(r)\}_{r=1}^n$ and it is understood that it may depend on the sequence \mathbf{r}_{s-1} of previous results. Hence, the optimal greedy average success probability at step s , can be written as

$$P_s^{\text{G}} = \sum_{\mathbf{r}_{s-1}} p(\mathbf{r}_{s-1}) \mathcal{P}_s^{\text{G}}(\mathbf{r}_{s-1}), \quad (76)$$

where the probability of successful identification of the change point at step s conditioned to the occurrence of the sequence \mathbf{r}_{s-1} [\mathcal{P}_s^{G} in Eq. (71); we recall that the dependence on \mathbf{r}_{s-1} is understood there] is

$$\begin{aligned} \mathcal{P}_s^{\text{G}}(\mathbf{r}_{s-1}) &= \max_{\{E_s(r)\}} \sum_{r=1}^n \max_k p(k | \mathbf{r}_{s-1}) \\ &\quad \times \langle \Psi_k | E_s(r) | \Psi_k \rangle, \end{aligned} \quad (77)$$

and we have used Bayes' rule to obtain the relation $(1/n)p(\mathbf{r}_{s-1} | k) = p(k | \mathbf{r}_{s-1})p(\mathbf{r}_{s-1})$. From Eq. (77), it is apparent that the optimal measurement can only depend on the updated priors $\eta_k^{(s)} := p(k | \mathbf{r}_{s-1})$, rather than on the whole sequence of previous results, as the maximization is only subject to the POVM conditions $E_s(r) \geq 0$ and $\sum_{r=1}^n E_s(r) = \mathbb{1}$. Likewise, the optimal guess can only depend on $\eta_r^{(s)}$ [Eq. (74) and the paragraph below it].

[2] M. Abramowitz and I.A. Stegun, *Handbook of Mathematical Functions* (Dover, New York, 1970).
[3] N. Dalla Pozza and G. Pierobon, Phys. Rev. A **91**, 042334 (2015).

[4] C.W. Helstrom, *Quantum Detection and Estimation Theory* (Academic Press, New York, 1976).